Synthesis and characterization of Nano-AgO particles by chemical reduction and antimicrobial activity against some selected bacteria.

Madan Kumar Gundala[1], G. Kalpana Ginne[2], Dr. M. Ravinder[2]* and Dr.M. Sujatha[1]*

*[1]Department of Chemistry, KoneruLakshmaiah Education Foundation, Guntur, Andhra Pradesh, India-522502

*[2] Chaitanya (Deemed to be University), Hanamakonda, Warangal, Telangana, India-506001.

Email ID: Sujatha.kluniversity@gmail.com

Abstract:

Here, silver oxide nanoparticles were made using the chemical reduction approach. We expect that the resulting nano-AgOparticles have a bactericidal effect on their mentioned Gram-positive and Gram-negative bacteria. We looked at the structural and morphological characteristics of nano-AgO particles, which are well known to be very toxic to both gram-negative and gram-positive microorganisms, including drug-resistant bacteria. The created nano-AgO particles were examined using a variety of methods, including Transmission Electron Microscopy (TEM), Scanning Electron Microscopy (SEM), Fourier Transforms Infrared spectroscopy (FTIR), and X-ray Diffraction spectroscopy (XRD). The characterization results for AgO NPs demonstrate aggregates of grains with a constrained size range, with individual particle radii ranging from 100 to 200 nm. The bactericidal activity of nano-AgO particles against *Pseudomonas aeruginosa (P. aeruginosa), Streptococcus pyogenes (S. pyogenes),* and *Klebsiella pneumoniae*was proven by well diffusion results within a 17 mm zone of inhibition.

***Keywords*:** Nano-Ag Oxide particles, Chemical reduction, FTIR, XRD, SEM, TEM, and Anti-Microbial activity.

1. Introduction:

Nanotechnology is a new field of research that has quickly gained recognition and traction in the scientific community during the past few years. Nanoparticles between 1 and 100 nm in size are considered. nano-AgO particlesstand out from the crowd of metallic nanoparticles thanks to their distinct physical, biological, and chemical properties [1,2]. When silver ions are converted into metal nano-AgO particlesusing chemical reduction (CR) techniques of synthesis, it is interesting to note that their toxicity decreases but their antibacterial capabilities significantly increase [3,4,5 and 6].Metal nanoparticles made through

a chemical process have been used in antimicrobials, treatments, and biomolecular detection and catalysis, among other fields[7]. It has been shown that silver nanoparticles on the nanometric scale (less than 200 nm) are very beneficial [8,9,10 and 11]. This is due to the high degree of surface development, which permits maximal interaction with the environment [12].

Many different top-down and bottom-up methods, including chemical reduction, may produce nano-AgO particles. Less expensive and less time-consuming chemical reduction techniques are thus often used [13,14]. By using sodium borohydride and other reducing agents, the concentration of Ag $(NO_3)_2$ may be lowered to an acceptable level [15].The chemical reduction procedure, which is the most popular technique for creating nanoparticles, uses an organic solvent like ethylene glycol [16] as well as reducing substances like hydrazine [17], sodium borohydride [18], trisodium citrate [19] and ascorbate [20]. A reducing agent is also used in this procedure. There was a critical need for the creation of processes that were safer and cleaner due to the low yield, complicated purification, and energy-intensive nature of chemical reduction.

There is still a lack of knowledge on the precise mechanism by which nano-AgO particlesinhibit bacterial growth. Several studies have shown that the nanoparticle's bactericidal activity of positively charged relies on its electrostatic attraction to negatively charged bacterial cells [21,22].This study aims to examine the antibacterial activity of CR-synthesized nano-AgO particlesagainst a wide range of Gram-negative and Gram-positive pathogens, such as *Pseudomonas aeruginosa*, *Streptococcus pyogenes*, and *Klebsiella pneumoniae*, using the antimicrobial test approach.

2. Experimental:

2.1 Materials:

To begin, we'll need 98 % pure Ag $(NO_3)_2$, 98 % pure $NaBH_4$ as the reducing agent, 98 % pure Sodium alginate as the stabilizing agent, 98 % pure THF as the solvent, and 99 % percent pure deionized water purchased from a local store. Analytical grade reagents are only available from S.D. Fine Chemicals.

2.2 Method:

2.2.1 Preparation of nano-AgO particles:

A technique called chemical reduction was used to create the nano-sized Silver Oxide particle [23]. We started by dissolving 0.1 M Ag $(NO_3)_2$ in 100 ml of deionized water to

fabricate nano-AgO particles. Now we have a 100 ml 0.1 M $NaBH_4$ solution that we made by dissolving $NaBH_4$ in THF. We finished by dissolving 100 ml of sodium alginate in deionized water to make a 10% solution.

50 ml of 0.1 M Ag $(NO_3)_2$ solution should be added to an RB flask. After that, you're supposed to put the flask at about 60° C to 70 ° C while stirring it regularly with a magnetic stirrer for approximately 1 Hr. This technique must be carried out despite the varying falling times and reaction temperatures. After adding 40 ml of a 0.1 M $NaBH_4$ solution, 25 ml of a 10% sodium alginate solution is added (10–15 minutes dropwise), while the mixture is stirred constantly. Now, heat the whole reaction mixture at a temperature of 50° C to 60 ° C using a magnetic stirrer for the next 120 minutes. The nano-AgO precipitate, from the initial yellowish-white to brown color, must now be removed.

3. Results and discussion:

3.1 Transmission Electron Microscopy (TEM):

The JOEL JEM-2200 FS 300 kV TEM evaluates the morphology and size of the nanoparticles. TEM works like a conventional microscope using electrons instead of light. It can gather nanoparticle data via diffraction and imaging. Sonicating a zinc-coated carbon grid in toluene creates nano-Ag oxide particles of the TEM sample for analysis. Before studying nano-AgO NPs, the TEM grid's film is dried in a fume hood for seven days. Then, the grid is put in a vacuum container,blotting paper removes the leftover solution.

Microscopic investigation of the CR reaction media revealed colloidal nano-AgO particles, The CR method of TEM micrographs indicates that nano-AgO particlesare distinct, spherical nanoparticles with little aggregation. Using ImageJ software and TEM, it was discovered that the precise size of the CR synthesized nano-AgO particleswas in the range of 200 nmshown in **Fig. 1 and 2**.Besides the conventional absorption-based imaging, the TEM may also see changes in chemical identity, crystal orientation, electronic structure, and sample-induced electron phase shift via the use of other modes of operation.

According to the data shown in **Fig. 3, and 4,** nano-zinc oxide particles have a spherical and cubic shape and an amorphous structure, and their average size is 200 nm. Previous studies showed evidence supporting this [24]. The CR method was revealed to be directly responsible for a decrease in particle size.

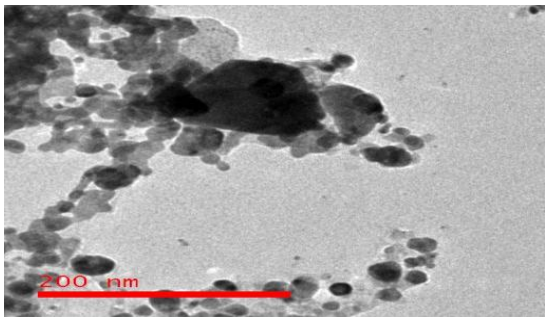

Figure-1

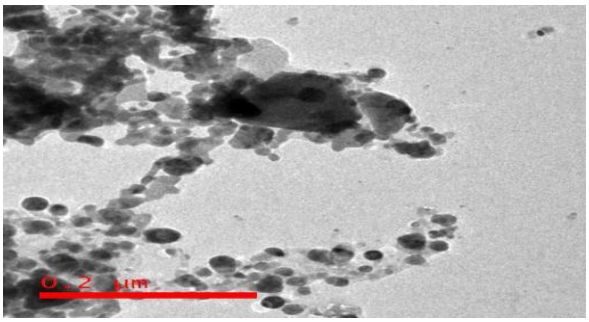

Figure-2

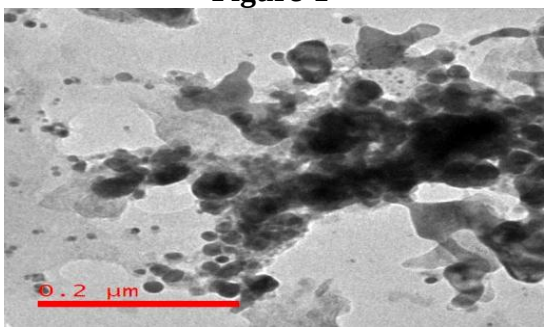

Figure-3

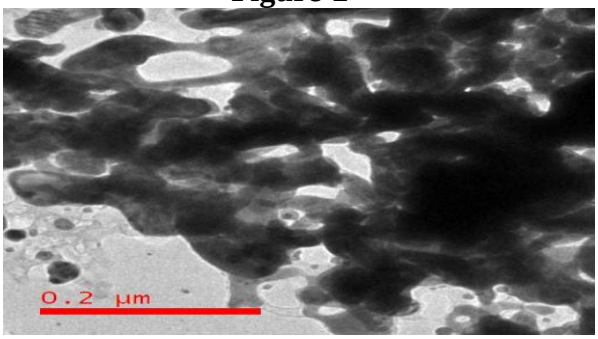

Figure-4

Fig.1,2,3, and 4. TEM-Images of Nano-Silver Oxide particles

3.2 Scanning Electron Microscopy (SEM):

It is impossible to estimate the size of each particle with TEM, which may be estimated using SEM. It is clear from the micrograph that the particles were irregular in shape, but further testing with a particle analyzer was necessary to identify the particles' exact size with TEM. The SEM was used to show three-dimensional images of NPs with high-resolution, multi-magnification. These discoveries of 3-D images are made using the scanning electron microscope (SEM; JEOL-JSM 5800) and a concentrated beam of high-energy electrons with multi-magnification (20X to 30000X).

The particle size was found to decrease with an increase in reaction temperature from 50°C -60°C. **Fig. 5 and 6**show an SEM picture of the precipitate and nanoscale nano-AgO particlespowder. This lines up with the comment that was supposedly made. nano-AgO particleswere observed to agglomerate, resulting in larger size particles, likely as a consequence of their high surface area and surface energy. In this study, it was shown that the average size of nano-AgO particlesin their crystalline state is between 100 and 200 nm. This is not a novel discovery, since it has been found by other researchers [25], an increase in magnitude is consistent with the presence of NPs. It is evident from the SEM images acquired using the CR method that the generated nano-AgO particleshave a wide range of surface morphologies **Fig. 7.** The SEM results show that the surface of the nano-AgO

particleshas a highly developed fine-grained structure, with granules ranging in size from 100 to 200 nm **Fig. 8.**

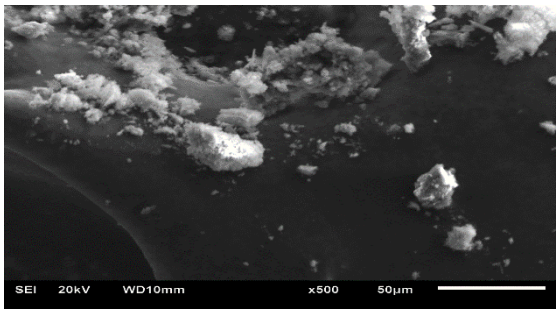

Figure-5

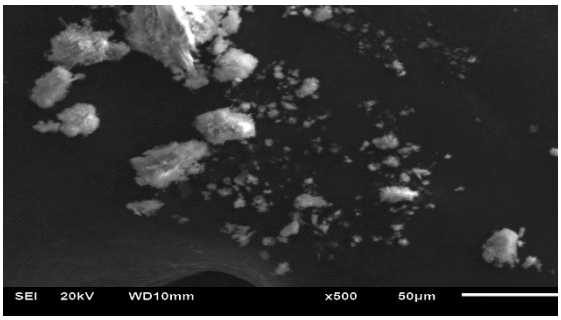

Figure-6

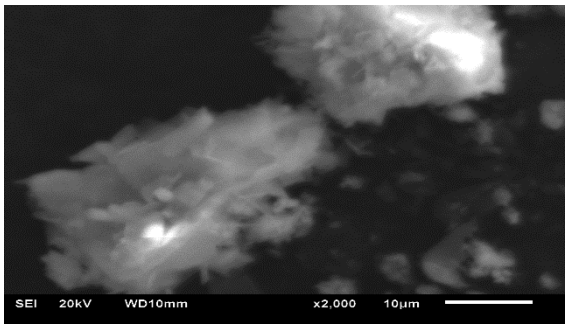

Figure-7

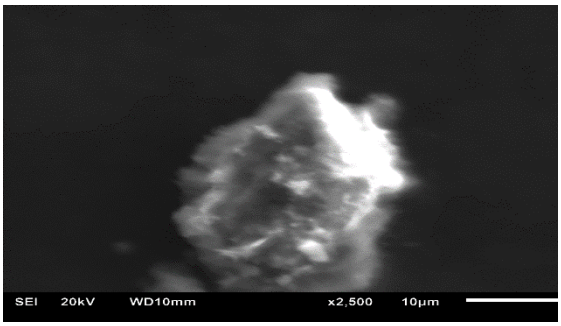

Figure-8

Fig.1,2,3, and 4. SEM-Images of Nano-Silver Oxide particles

3.3 X-Ray Diffraction (XRD):

The quantitative, versatile, and corrosion-free X-ray diffractometer can accurately determine the phase of any crystalline material. The sizes and measurements of the unit cells are provided. To learn more about Nano-Ag Oxide, we may use XRD (XPERT-PRO model X-ray diffraction) equipment operating at 45 kV, 40 mA, and Cu Kα radiation in a θ - 2θ configuration. The average bulk composition of homogenized and finely milled powdered Nano-Ag Oxide materials is evaluated using a monochromatic X-ray picture.

To further understand the crystalline nature of the particles, an XRD analysis was performed on nano-AgO particlesgenerated by the CR method using Ag $(NO_3)_2$. An XRD pattern representative of CR-synthesized AgO NPs is shown as an example in **Fig. 9**. The data shows that there are four diffraction peaks at 2θ of 38.2°, 44.1°, 64.1°, and 77.0°, Matches were made between angles and their corresponding planes, such as (111), (200), (220), and (311). However, the average crystalline size of the nano-AgO particlessynthesized using CR was found to be 200 nm using the Debye-Scherrer equation. Distinguishing between diffraction peaks is made feasible by the presence of nano-crystalline AgO. **Fig. 9** demonstrates that the samples have reached a monocrystalline state, with nanoparticles of silver oxide favoring preferred orientations (111) and (200). The identical diffraction peaks and crystalline properties

were also detected in a recent study describing the characterization of eco-friendly CuO NPs [26]. X-ray diffraction analysis of a reference sample of nano-AgO particlesshowed two broad signals at 38.2° and 44.1°, showing that the silver nanoparticles are crystalline, face-cantered, and cubic in shape.

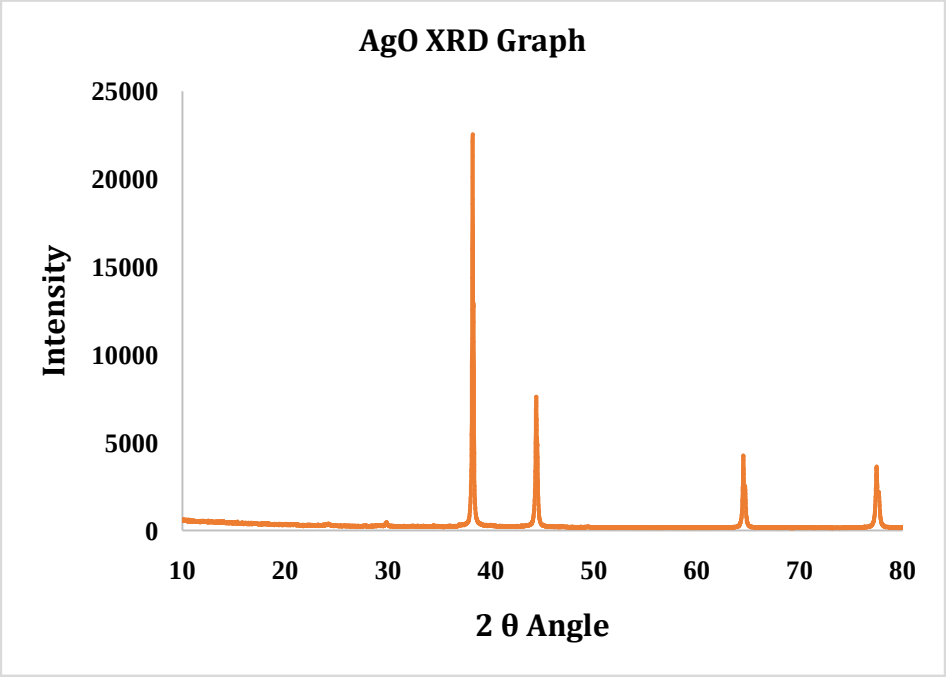

Fig.9. X-ray Diffraction graph of Nano-Silver Oxide particles

3.4 FTIR (Fourier transform infrared) Spectroscopy:

The stretching and bending vibrations of Nano-Ag Oxide bonds are measured using FTIR spectroscopy at different frequencies (Hz). Multiple excited states are produced as bond vibration increases, and these states may be identified by observing the electromagnetic radiation that is emitted. The change is clear. FTIR can examine solids, gases, and liquids to uncover novel combinations. The 400 cm^{-1} to 4000 cm^{-1} range and 4 cm^{-1} resolution are provided by the Bruker ALPHA-T Version model. These factors enable it to provide wavelength and transmittance spectra.

To determine if the synthesized metal nano-AgO particle is properly stabilized and to determine its composition, FTIR studies were carried out. **Fig.10** demonstrates the presence of a shoulder peak at 1660.42 cm^{-1} and a prominent band typical of nano-AgO particles at 2359.94 cm^{-1}. The O-H bending vibration of physically adsorbed water is seen at 3424.78 cm^{-1} in one of the distinctive bands. An additional identifying spectrum it is possible to think of the characteristic band at 2925.76 cm^{-1} as the stretching vibration mode of C=O, this band was

likely produced by water vapor and carbon dioxide in the atmosphere. Since silver nitrate contains the nitronium ion, the absorption band at 1384.11 cm^{-1} indicates the presence of nitrogen dioxide (NO_2). A C-C single bond stretching vibration was possible, according to the solvent's 1274.84cm^{-1}peaks. Weak C-H bending vibrations are represented by peaks between 917.61 cm^{-1} and 717.94cm^{-1}, while weak O-H bending vibrations are represented by peaks between 669.98 $cm^{-1}$and 457.17 cm^{-1}. The synthesized nano-AgO particles' FTIR analyses demonstrate that their preparation has been effective in evaluating this prospective investigation.

Table 1 Standards of FTIR spectroscopy:

S.No	IR values of Nano-Ag oxide	Obligation
1.	1660.42 cm^{-1}	Shoulder peak of silver
2.	2359.94 cm^{-1}	Strong AgO band
3.	3424.78 $cm^{-}1$	O-H bending vibrations
4.	2925.76 cm^{-1}	C=O Stretching vibrations
5.	1384.11cm^{-1}	NO_2 stretching vibrations
6.	1274.84cm^{-1}	C-C single bondstretching vibrations
7.	917.61 cm^{-1} and 717.94 cm^{-1}	Weak C-H bending vibrations
8.	669.98 $cm^{-1}$and 457.17 cm^{-1}	Weak O-H bending vibrations

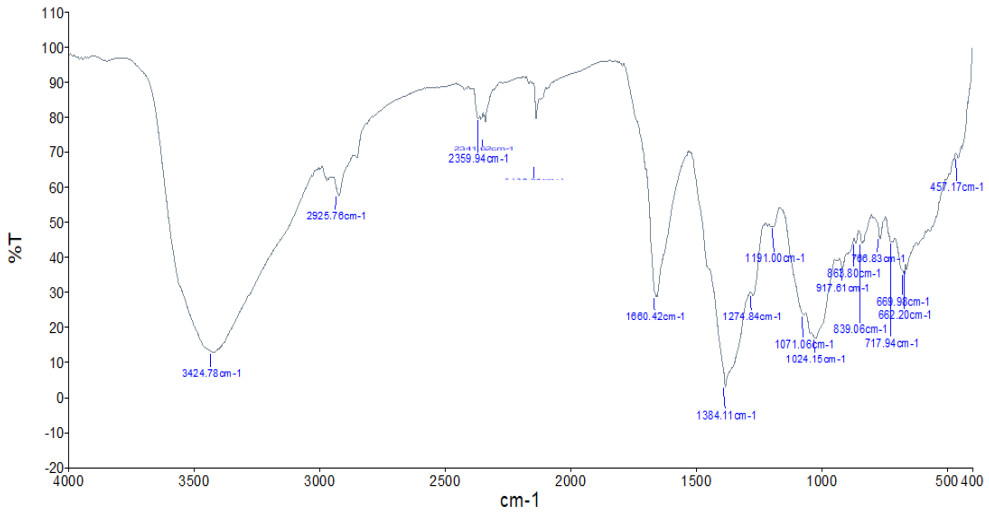

Fig.10. FTIR Graph of Nano-AgO particles

3.5. Anti-Microbial Activity:

The antibacterial activity of nano-AgO particles was examined using the disc diffusion method against both Gram-negative and Gram-positive pathogens, including *P. aeruginosa, S. pyogenes,* and *Klebsiella pneumoniae*. The results demonstrated that nano-AgO particles are effective in killing Gram-negative bacteria. After adding 10^7 colony-forming units (CFU) to 1 ml of the final inoculate, which included about 10^8 colony-forming units of the bacteria, equal portions of each sample were added to the mixture. Distilled water was used to dissolve the Mueller-Hinton Broth ingredients before they were transferred to sterile microtubes.

The strains of Gram-positive and Gram-negative bacteria (*P. aeruginosa, S. pyogenes,* and *Klebsiella pneumoniae*) were cultivated in Mueller Hinton broth (MHB) at 37 °C for 24 hours with 200 rpm agitation. Then, using distilled water, we create solutions with various concentrations of nano-AgO particles. Their molecular weights vary from 0.0012, 0.0024, 0.0037, 0.0049, 0.0061, 0.0074, 0.0086, 0.0096, 0.0111,and 0.0123, and these concentrations are equal to within milligrams of 10, 20, 30,40, 50, 60, 70, 80, 90, and 100.

Three different bacterial strains on MHB agar Petri plates were exposed to solutions containing nano-silver oxide at varied concentrations. We raised a reaction mixture devoid of nano-Ag Oxide particles in the MHB plate well under the same circumstances as the control test. Three MHB Petry plates are incubated for 24 hours at 37°C before the inhibitory zone is measured.

The inhibitory zone measurements for *P. aeruginosa*were mm 1.5, 2.8, 4.3, 7.2, 9.8, 12, 15.5, 17.2, 20.5, and 22 at 10, 20, 30, 40, 50, 60, 70, 80, and 90 mg. The inhibition zone values for *S. pyogenes*start from 10 mg and values are 1.0, 4.5, 7.5, 9.7, 11.5, 13.4,15.2, 17, 18.3, and 11 mm for the same concentrations of nano-AgO solution.The inhibition zone values for *Klebsiella pneumoniae*also start from 10 mg and are as follows: 0.4, 0.8, 1.7, 2.1, 3.4, 5.5, 7.2, 10.3,12.5, and 14 mm for the above-mentioned same concentrations of nano-AgO solutions. According to the findings, *P. aeruginosa* is the most vulnerable bacterium to Nano-AgO particles' strong antibacterial effects (as seen in **Fig. 11, 12, and 13**). It is clear that at the same dosage of AgO NPs, Gram-negative bacteria like *P. aeruginosa*display a larger zone of inhibition than Gram-positive bacteria like *S. pyogenes* and *Klebsiella pneumoniae* and the values are shown in the **table. 2**

Table 2. Zone of inhibition standards of Anti-Microbial activity:

S. No	Conc. of Nano-AgO	Zone of inhibition in mm

	In Moles	In mg	*Pseudomonas aeruginosa*	*Streptococcus pyogenes*	*Klebsiella pneumoniae*
1.	0.0012	10	1.5	1.0	0.4
2.	0.0024	20	2.8	4.5	0.8
3.	0.0037	30	4.3	7.5	1.7
4.	0.0049	40	7.2	9.7	2.1
5.	0.0061	50	9.8	11.5	3.4
6.	0.0074	60	12	13.4	5.5
7.	0.0086	70	15.5	15.2	7.2
8.	0.0096	80	17.2	17	10.3
9.	0.0111	90	20.5	18.3	12.5
10.	0.0123	100	22	19	14

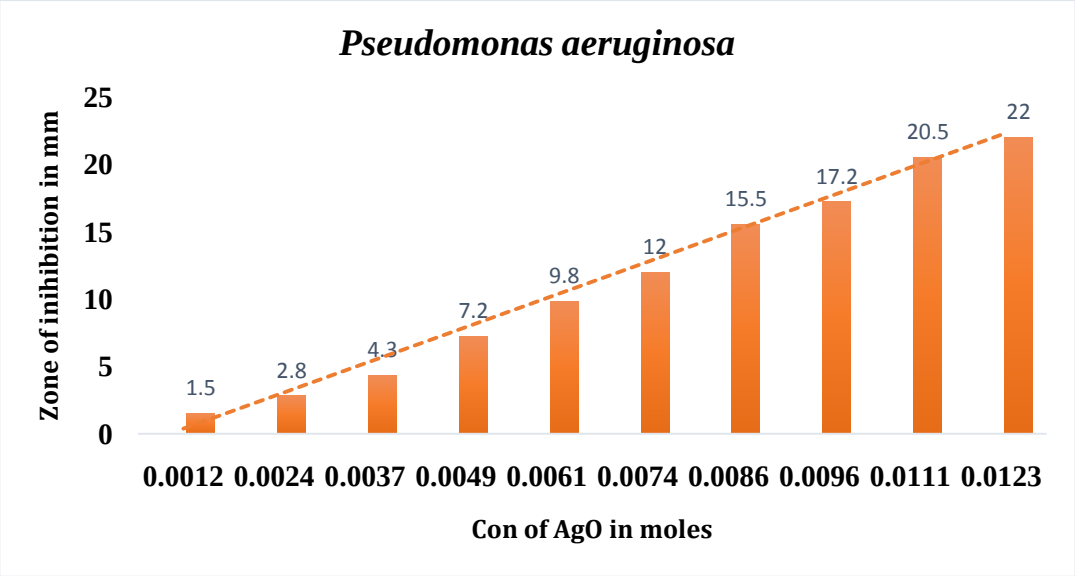

Fig.11. Graph of Anti-Microbial activity with *P. aeruginosa*

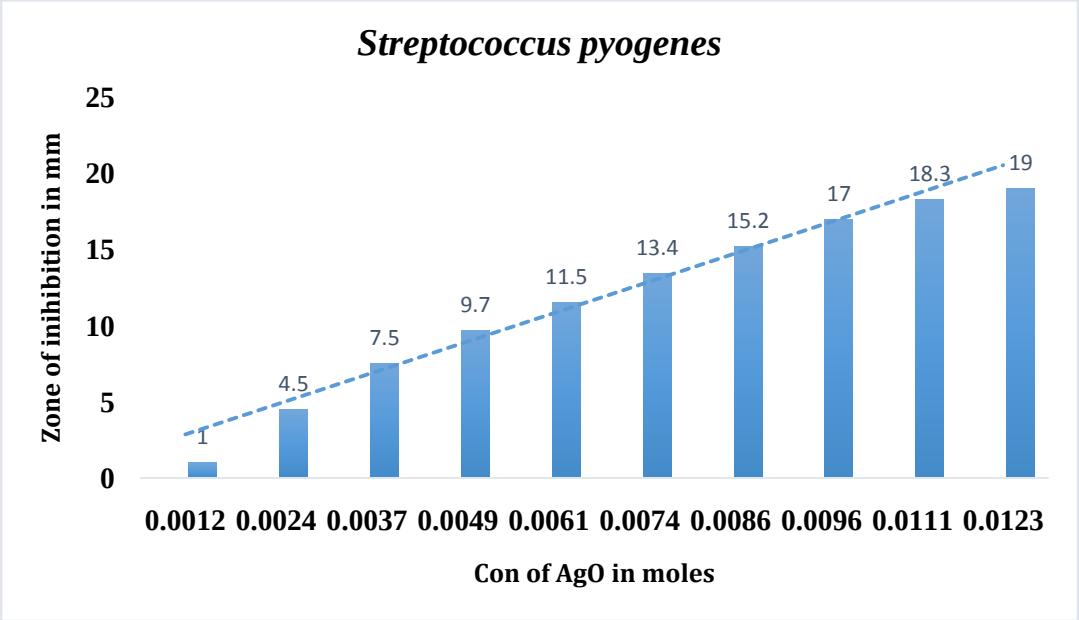

Fig.12. Graph of Anti-Microbial activity with *S. pyogenes*

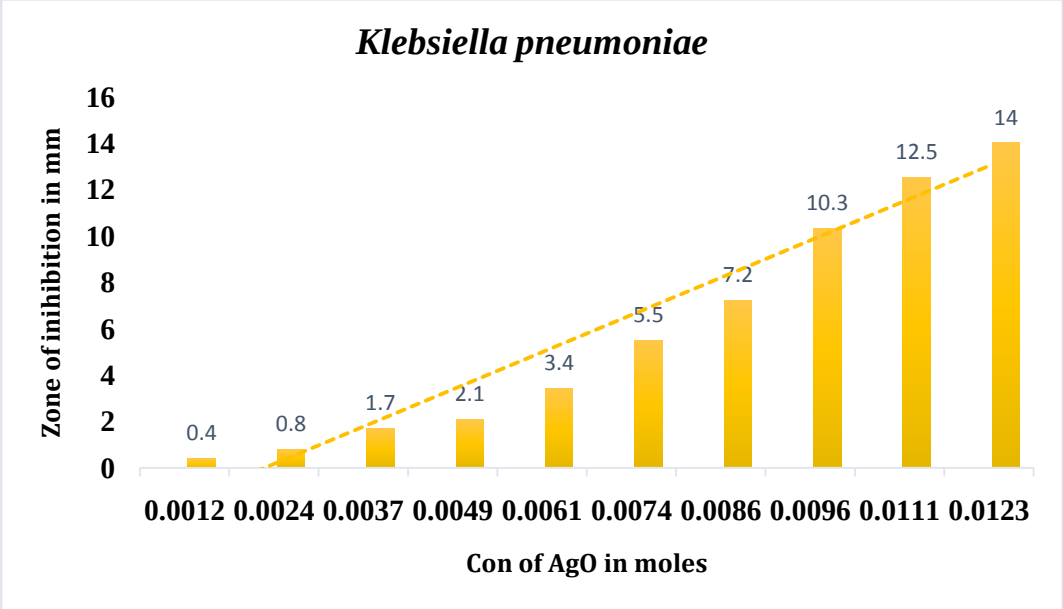

Fig.13. Graph of Anti-Microbial activity with *Klebsiella pneumoniae*

4. Conclusion:

We have shown a straightforward CR method for generating nanoscale AgO particles from an aqueous solution of Ag $(NO_3)_2$. In both TEM and SEM imaging, nano-AgO particles with a size of less than 200 nm have been discovered. Several physicochemical characterization methods validated the effective production of nano-AgO

particles in spherical, face-cantered, and cubic geometries, including XRD and FTIR. The effectiveness of the nano-AgO particle dispersion against bacteria was also evaluated using the disc diffusion technique.

This study's findings showed that the examined Gram-negative and Gram-positive pathogens, including *Pseudomonas aeruginosa, Streptococcus pyogenes, and Klebsiella pneumoniae*, were all hindered in their development and multiplication by the colloidal nano-AgO particles. This is because nano-AgO particles in combination with antibiotics are effective against many drug-resistant bacteria and may be used as conveniently accessible therapy. Consequently, nano-AgO particles may be an attractive option to develop as an antibacterial agent against the aforementioned pathogens that cause illnesses including UTIs, pneumonias, IAIs, BSIs, scarlet fevers, septicemias, and bloodstream infections caused by multidrug-resistant bacterial strains.

5. Conflicts of interest:

"In this case, there is no possibility for conflicts of interest that should be disclosed".

6. Acknowledgment:

Thanks to the Research Center of the *KoneruLakshmaiah Education Foundation* Department of Chemistry and the Research Center of the *Chaitanya (Deemed to be University)* Department of Chemistry, the authors were able to conduct their research.

References:

1. G. Franci,A. Falanga, V. Galdiero, Z. Palomba,V. Rai, and V. Morelli, Silvernanoparticlesaspotentialantibacterialagents. *Molecules.*,20(5), 8856–8874 (2015)., DOI:10.3390/molecules20058856.
2. V. Harish, M.M. Ansari, D. Tewari, M. Gaur, A.B. Yadav, M-L. García-Betancourt, F.M Abdel-Haleem, M. Bechelany, A. Barhoum, Nanoparticle, and Nanostructure Synthesis and Controlled Growth Methods. *Nanomaterials*., 12, 3226. (2022) DOI: 10.3390/ nano12183226
3. K. Jadhav, D. Dhamecha, D. Bhattacharya, M. Patil, eco-friendlysynthesis of silver nanoparticles: characterization, biocompatibility studies and gelformulation for treatment the of infections in burns.*J. Photochem.*, S1011-1344(15)30162 (2016)., DOI: 10.1016/j.jphotobiol.2016.01.002
4. H. Aritonang, H. Koleangan and A. Wuntu, Synthesis of Silver Nanoparticles Using

Aqueous Extract of Medicinal Plants' (Impatiens balsamina and Lantana camara) Fresh Leaves and Analysis of Antimicrobial Activity. *Int. J. Microbiol*., 2019 (8642303), 8 pages DOI:10.1155/2019/8642303

5. J. Mussin, & G. Giusiano, Product Validation Process Based on Traditional Knowledge of Medicinal Plants. in Agricultural, *Ethno–Phytopharmacology*., 331–353 (2020)., DOI: 10.1007/978-3-030-51358-0_17
6. D. Jini, S. Sharmila, Green synthesis of silver nanoparticles from Allium cepa and it's in vitro antidiabetic activity. *Mater. Today Proc*. 22, 432–438 (2020)., DOI: 10.1016/j.matpr.2019.07.672
7. A. Iqbal, A., A.S. Ahmed, N. Ahmad, A. Shafi, T. Ahamad, M.Z. Khan, S. Srivastava, Biogenic synthesis of CeO2 nanoparticles and its potential application as an efficient photocatalyst for the degradation of toxic amido black dye. *Environ. Nanotechnol. Monit. Manag.* 16 (2021) 100505., DOI: 10.1016/j.enmm.2021.100505.
8. P. Christopher, H. Xin, S. Linic, Visible-light-enhancedcata-lyticoxidationreactionsonplasmonicsilvernanostructures.*Natu. Chem.*,3(6), 467-472 (2011)., DOI: 10.1038/nchem.1032
9. S. Sadhasivam, P. Shanmugam, K. Yun, Biosynthesisofsilver nanoparticles by Streptomyces hygroscopic and antimicrobial activity against medically important pathogenic microorganisms.*Colloids Surf. B.*,81(1), 358–362 (2010)., DOI: 10.1016/j.colsurfb.2010.07.036.
10. R. Kumari, R.C. Mishra, J.P. Yadav, Antioxidant and cytotoxic studies of Acacianiloticatwigextractandtheirgreensynthesizedsilvernanoparticles.*Lett.Appl. Nanobiosci*.9,975–980., DOI:10.33263/LIANBS92.975980.
11. Hussain, Mohamed Hasaan; Abu Bakar, Noor Fitrah; Mustapa, Ana Najwa; Low, Kim-Fatt; Othman, Nur Hidayati; Adam, Fatmawati. Synthesis of Various Size Gold Nanoparticles by Chemical Reduction Method with Different Solvent Polarity Nanoscale *Res. Lett.*, 15(1), 140– (2020). DOI: 10.1186/s11671-020-03370-5.
12. YA. Krutyakov, AA. Kudrinskiy, AY. Olenin. GV. Lisichkin, Synthesis,andPropertiesofSilverNanoparticles:Advances and Prospects. *Russian Chem Re;* 77(3), 233-257 (2008)., DOI:10.1070/RC2008v077n03ABEH003751
13. A.Zieliń ska,E.Skwarek,A.Zaleska,M.Gazda,andJ.Hupka, Preparation of silver nanoparticles with controlled particlesize.*ProcediaChemistry.*,1(2),1560–1566 (2009).
14. G. Marslin, K. Siram, Q. Maqbool, et al., "Secondary metabolites in the green synthesis of

metallic nanoparticles," *Materials*, 11 (6), 940 (2018)., DOI: 10.3390/ma11060940.

15. Sondik and S. Salopek-Sondi, Silver nanoparticles as antimicrobialagent:acasestudyonE.Coliasamodelforgram-negative bacteria. *J. Colloid Interface Sci*., 275(4),177–182 (2004)., DOI: 10.1016/j.jcis.2004.02.012
16. B. Wiley, T. Herricks, Y. Sun, and Y. Xia, Polyol synthesis of Silver nanoparticles: Use of chloride and oxygen promote the formation of single-crystal, truncated the formation cubes, and tetrahedrons.*NanoLett.*, 4(9), 1733–1739 (2004)., DOI: 10.1021/nl048912c
17. MG. Guzmán, J. Dille, S. Godet, Synthesis of Silver nanoparticles by chemical reduction method and their antimicrobial activity, *Int*.*J.Chem.BiomolEng.*, 2(3), 104–11 (2009)., DOI; scholar.waset.org/1307-6892/6289.
18. KC. Song, S.M. Lee, T.S. Park, Preparation of colloidal silver nanoparticles by chemical reduction method, *KoreanJ ChemEng.*, 26(1), 153–5 (2009)., DOI: 10.1007/s11814-009-0024-y.
19. MU. Rashid, MKH.Bhuiyan, ME, Quayum synthesis of silver nanoparticles (Ag-NPs) and their uses for Quantitative analysis of Vitamin C tablets.*J.PharmSci.*,12(1), 29–33 (2013)., DOI: 10.3329/dujps. v12i1.16297
20. X. Ji, J. Jing, H. Liu, H. Wu, W. Yang,Size control over silver nanoparticles by ascorbic acid reduction. *ColloidsSurfaPhysicochem.Eng.Asp.* 372(1-3), 172-176 (2010)., DOI: 10.1016/j.colsurfa.2010.10.013
21. T. Hamouda, Jr.Baker, Antimicrobialmechanismofactionofsurfactant lipid preparations in enteric gram-negative bacilli.*J. Appl.Microbiol.*, 89, 397-403 (2000)., DOI: 10.1046/j.1365-2672.2000. 01127.x
22. I. Sondi, B. Salopek-Sondi, Silvernanoparticlesasantimicrobialagent:acase study on E. coli as a model for gram-negative bacteria. *J. Colloid.Interface.Sci.*, 275 (1), 177-82 (2004)., DOI: 10.1016/j.jcis.2004.02.012
23. L. Wang, M. Muhammed, Synthesis of zinc oxide nanoparticle with controlled morphology. *J. Mater Chem.*, 9 (11), 2871-2878 (1999)., DOI: 10.1039/A907098B.
24. L.K. Jangir, Y. Kumari, A.Kumar, M. Kumar, K.Awasthi, Investigation of luminescence and structural propertiesofZnOnanoparticles,synthesizedwithdifferentprecursors. *Mater.Chem.Front*.,1, 1413–1421 (2017). DOI: 10.1039/C7QM00058H
25. C.H. Lu, C.H. Yeh, Influence of hydrothermal conditions on themorphology and particle size of zinc oxide powder. *Ceram. Int.*, 26 (4), 351–357 (2000)., DOI:10.1016/S0272-8842(99)00063-2

26. D. O. B. Apriandanu, Y. Yulizar,Tinosporacrispa leaves extract for the simple preparation method of CuO nanoparticles and its characterization.*Nano-Struct.Nano-Objects*., 20, 100401 (2019)., DOI:10.1016/j.nanoso.2019.100401